RSC Advances

REVIEW

View Article Online
View Journal | View Issue

Cite this: *RSC Adv.*, 2018, **8**, 10040

A review on organic–inorganic hybrid nanocomposite membranes: a versatile tool to overcome the barriers of forward osmosis

Wanying Sun,† Jie Shi,† Cheng Chen, Nan Li, Zhiwei Xu,* Jing Li, Hanming Lv, Xiaoming Qian and Lihuan Zhao

Forward osmosis (FO) processes have recently attracted increasing attention and show great potential as a low-energy separation technology for water regeneration and seawater desalination. However, a number of challenges, such as internal concentration polarization, membrane fouling, and the trade-off effect, limit the scaleup and industrial practicality of FO. Hence, a versatile method is needed to address these problems and fabricate ideal FO membranes. Among the many methods, incorporating polymeric FO membranes with inorganic nanomaterials is widely used and effective and is reviewed in this paper. The properties of FO membranes can be improved and meet the demands of various applications with the incorporation of nanomaterials. This review presents the actualities and advantages of organic–inorganic hybrid nanocomposite FO membranes. Nanomaterials applied in the FO field, such as carbon nanotubes, graphene oxide, halloysite nanotubes, silica and Ag nanoparticles, are classified and compared in this review. The effects of modification methods on the performance of nanocomposite FO membranes, including blending, *in situ* interfacial polymerization, surface grafting and layer-by-layer assembly, are also reviewed. The outlook section discusses the prospects of organic–inorganic hybrid nanocomposite FO membranes and advanced nanotechnologies available for FO processes. This discussion may provide new opportunities for developing novel FO membranes with high performance.

Received 27th November 2017
Accepted 26th February 2018

DOI: 10.1039/c7ra12835e

rsc.li/rsc-advances

1. Introduction

Forward osmosis (FO) is a promising membrane separation technology with recently expanded focus as a low energy process.[1,2] It is a spontaneously occurring osmotic process that separates water effectively from a dissolved solute *via* a semi-permeable membrane. Unlike conventional pressure-driven membrane processes, FO is driven by osmotic pressure between the feed solution and draw solution.[3] Without external pressure, the FO process has several unique benefits, including low energy consumption, low operating cost, efficient separation and a wide range of feed solutions.[4–6] Therefore, FO is deemed to be potentially useful in various industries, such as desalination, waste water treatment,[7] food processing, medicine, and biological processes.[8,9] A desirable FO membrane must possess high water flux and solute rejection, low concentration polarization, adequate mechanical and antifouling properties and good stability. However, some drawbacks still limit the application of FO in large scale processes. The most severe of these include: (1) internal concentration polarization (ICP); (2) membrane fouling; (3) the trade-off effect. To address these limitations, many efforts have been made to improve conventional FO membranes, among which organic–inorganic hybrid nanocomposite FO membranes are a candidate to mitigate these problems.

ICP is one of the most serious problems in FO processes; it dramatically reduces the osmotic driving force. Hence, the water flux declines and negatively affects the FO process. In order to minimize ICP, FO membranes should have low structural parameters. Hydrophilicity and wettability modifications of the FO support layers are the main methods of ICP mitigation. It is assumed that a hydrophilic support layer not only promotes the transport of water and solute molecules, but also enhances the wettability of the support layer. Hence, hydrophilization of the FO support layer is an active area of membrane research. Many studies have found that the incorporation of nanomaterials can significantly enhance the hydrophilicity of FO membranes. Also, incorporation of nanomaterials into the support layer of FO membranes promotes decrease of the structural parameter, which implies a lower ICP. Ma *et al.*[10] incorporated zeolite into the polysulfone support layer of an FO membrane to obtain a lower ICP. The resulting membrane had a decreased structure parameter from 0.96 mm

State Key Laboratory of Separation Membranes and Membrane Processes, School of Textiles, Tianjin Polytechnic University, Tianjin 300387, China. E-mail: xuzhiwei@tjpu.edu.cn; Fax: +86 022 83955231; Tel: +86 022 83955231

† These authors contributed equally to this work.

to 0.34 mm and increased water flux. This result was attributed to the higher porosity, enhanced hydrophilicity and additional water channels supplied by the addition of porous zeolite. This was the first study to exhibit the feasibility of employing an organic–inorganic hybrid nanocomposite FO membrane to limit ICP in the FO process. Subsequently, researchers have used multi-walled carbon nanotubes (MWCNTs)[11–13] and TiO_2 (ref. 4, 14 and 15) to control ICP in the support layers of FO membranes. The resulting nanomaterials all demonstrated decreased structure parameters. Furthermore, the support layers also showed enhanced strength and other desirable properties for FO applications.

Membrane fouling is a complex procedure which has a strong impact on the performance of membranes, especially their filtration efficiencies and service life. Among fouling factors and mechanisms, some are universal in pressure-driven membrane processes, such as hydrodynamic conditions, membrane materials, feed solution constituents and concentration polarization. Other factors are specific to FO, such as the draw solution constituents, operating orientation of the membranes, and reverse diffusion. Although the membrane fouling of FO is reversible,[16] it is still considered to be a limitation that reduces the FO filtration efficiency, particularly for wastewater purification applications without pretreatment.[17] Many researchers have indicated that introducing nanomaterials into the active layer of a FO membrane will provide a smoother and more hydrophilic surface so that membrane fouling can be effectively prevented. It was discovered that with the incorporation of hydrophilic mesoporous carbons into their active layers,[18] FO membranes demonstrated increased surface hydrophilicity. A similar phenomenon was also observed by Zhao *et al.*[19] when they employed a hybrid nanocomposite FO membrane incorporated with MWCNTs.

The trade-off effect between permeability and selectivity is a barrier to the development of membranes. It is common knowledge that for conventional polymeric membranes, water flux and solute rejection cannot be increased simultaneously. To overcome the permeability/selectivity trade-off effect, permeability must be enhanced without sacrificing solute rejection. According to the published literature, higher rejection involves a combination of steric and Donnan exclusion.[20] Also, certain elements will disrupt this effect, such as reducing polymer cross-linking, increasing the surface charge density and providing adequate nanovoids and channels. For example, zeolite molecular sieves and silica nanoparticles can provide water pathways and enhance charge density. Hence, incorporating nanomaterials will affect polymer cross-linking and also provide adequate pathways to water rather than solutes, thus overcoming the trade-off effect.

As discussed above, incorporation of inorganic nanomaterials is a versatile method to modify FO membranes which can address the main problems that restrict the development of FO. Currently, with the development of membranes in water treatment and other fields, the requirements of membrane function, such as permeability, selectivity, anti-pollution, and chemical and thermal stability, are becoming more strict. It is difficult for traditional membrane materials to meet application requirements. Therefore, researchers have begun to turn their focus to developing novel composite membranes or membrane materials with suitable properties. The treatment and purification of water will benefit from improving the separation efficiency of membranes, and the water supply will be enhanced with safer water sources. Since Ma *et al.*[21] incorporated NaY zeolite nanoparticles into a polyamide active layer in 2012, recent advances in nanotechnology have offered opportunities for the development of FO technology. Fig. 1 shows the growing trend of published papers on organic–inorganic hybrid nanocomposite FO membranes.

In this work, we review the development of organic–inorganic hybrid nanocomposite FO membranes. We discuss the available nanomaterials, properties, advantages and modification methods used in the application of nanotechnology to the FO process. Diagrams of frequently used nanomaterials in the FO membrane field are summarized and presented in Table 1. In the last section, we list the limitations of this technique for commercialization and provide an overview of the trends in the development of nanocomposite FO membranes. By discussing these advanced technologies and the physicochemical properties of nanomaterials, this review outlines the opportunities and limitations to further capitalize on the unique properties of FO technology.

2. Effects of nanomodifiers on FO membrane performance

Currently, with the development of nanotechnology, many novel functional nanomaterials are being explored to enhance the performance of membranes. Employing inorganic nanomaterials with FO membranes can result in enhanced separation performance and the development of new functions, such as antisepsis and photocatalysis, that are endowed by the nanomaterials. Researchers have indicated that organic–inorganic hybrid nanocomposite membranes have significantly higher water flux, mechanical strength, selectivity, stability and hydrophilicity compared with conventional polymeric FO membranes.[22–24] The main objectives of incorporating inorganic nanomaterials into FO membranes are obtaining ideal

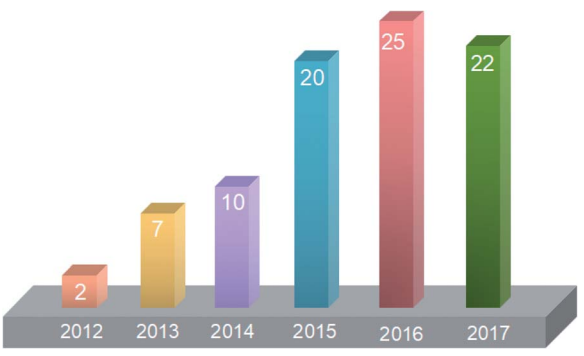

Fig. 1 Annual number of publications on organic–inorganic hybrid nanocomposite FO membranes since 2012. The data were obtained from Web of Science on 18th November 2017.

Table 1 Diagrams of the nanomaterials

Nanomaterial shape	Diagram	Nanomaterials
Tubular		CNTs, HNTs
Ball		Ag, TiO_2, SiO_2
Flake	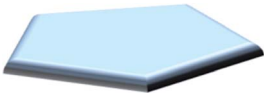	GO, zeolite
Massive		Boehmite, $CaCO_3$
Linear		CNFs

structures to mitigate ICP, reducing membrane fouling and overcoming the trade-off effect. The interactions between nanomaterials and polymer molecular linkers and the functional groups of nanomaterials are the major cause of enhanced performance.[25–28] Hence, organic–inorganic hybrid nanocomposite FO membranes with comprehensive performance can replace conventional polymeric FO membranes to meet the requirements of specific application areas. Table 2 summarizes nanomaterials composited with FO membranes and the filtration performance of the FO membranes.

2.1 Low-dimensional carbon-based nanomaterials

In recent years, low-dimensional carbon-based nanomaterials such as carbon nanotubes (CNTs) and graphene oxide (GO) have drawn great attention from scholars worldwide. Low-dimensional carbon-based nanomaterials with abundant oxygen functional groups and high surface areas have shown a series of unique advantages in environmental engineering, such as facile organization and hydrophilic modification. Carbon-based nanomaterials are considered to be the principal element of nanotechnology to enhance membrane performance.[50] Employing carbon-based materials in membrane preparation has recently become popular due to their unique properties, such as high specific surface area and smooth water channels.[51]

2.1.1 Carbon nanotubes. Since their discovery, CNTs have gained increasing attention due to their inner hollow cavities, which are similar to aquaporins. CNTs are composed of graphite lamellae rolled into columns.[52–54] Due to their unique characteristics, such as high aspect ratios, molecularly smooth surfaces, nanoscale diameters and inner hollow cavities, CNTs are ideal candidates in various fields,[55–58] particularly separation technology. Water molecules travel through the ultra-efficient molecular pipes orders of magnitude faster than through other pores of comparable size.[59] This phenomenon is mainly due to the super-hydrophobic and smooth graphitic walls of CNTs, which offer nearly frictionless pathways for water flow. When CNTs are blended into polymer membranes, the additional pathways induced by CNTs and the nanoslits between the CNTs and polymers enhance the permeability of membranes.[8] Moreover, CNTs have excellent bactericidal capabilities; they can destroy cytomembranes and disrupt the metabolic pathways of microorganisms.[60] It has been widely reported that the permeability, antifouling capacity and mechanical strength of a membrane will significantly increase upon incorporation of CNTs.[61–63] Although their high cost limits the large scale industrialization of CNTs, it is expected that this cost will decrease as the technology matures. CNTs represent promising building blocks in a number of industrial applications in the future.[64]

Because CNTs show extraordinary performance and appear to be less susceptible to ICP,[65] the possibility of incorporating CNTs into FO membranes has been investigated by several researchers.[61,66–68] In 2010, Wang *et al.*[30] synthesized a polyethersulfone/MWCNTs substrate for FO membranes. This was the first time that CNTs were blended into FO membranes. The results demonstrated that incorporating MWCNTs improved both the salt rejection and water permeability of FO membranes.

It is worthwhile to note that the main limitation of employing CNTs in polymeric membranes is their high hydrophobicity and low solubility in solution. Hence, surface functionalization of CNTs is needed to enhance their solubility in solution.[69] Amini *et al.*[8] fabricated amino MWCNTs and blended them in a 1,3-phenylendiamine aqueous solution to fabricate a nanocomposite active layer. The water flux and rejection of the resulting membranes improved. With increasing concentration of functionalized MWCNTs, the surface hydrophilicity of the membranes improved in aqueous solution. Similarly, Kunli Goh *et al.*[3] functionalized MWCNTs with immobilized polyethyleneimine–poly(amide–imide) hollow fiber membranes. The results indicated that the fabricated membranes incorporated with MWCNTs showed good properties, including enhanced water permeability without obvious impact on the rejection.

Song *et al.*[29] suggested a novel method to fabricate high performance FO membranes. They designed double-skinned membranes, which showed excellent solute rejection, and incorporated polydopamine with CNTs as the active layer by interfacial polymerization. They found that the CNTs had significant effects on the characteristics of the fabricated membranes. Therefore, it can be concluded that hybrid nanocomposite membranes incorporated with CNTs have higher FO water flux and remarkable antifouling capacity compared to conventional membranes.

Entangled CNTs with high flexibility[70,71] and mechanical stiffness form a nonwoven network structure that is known as bucky-papers. Bucky-papers have high tensile moduli (over 1 GPa)[72] and porosity.[72,73] Bucky-papers can be readily assembled and form ultrathin lamellae from any grade of CNTs. Although

Table 2 Summary of organic–inorganic hybrid nanocomposite FO membranes

	Nanomodifier	Polymer	Component loading	Test temperature	FS	DS	Operating orientation	Water flux	Solute flux	Reference
Low-dimensioal carbon based nanomaterials	CNTs	Polysulfone	0.01, 0.05 and 0.1 wt%	—	10 mM	2 M	FO	37 L m^{-2} h^{-1}	2.7 g m^{-2} h^{-1}	8
							PRO	95.7 L m^{-2} h^{-1}	5.2 g m^{-2} h^{-1}	
		Polyethyleneimine–poly(amide–imide)	0.31, 0.62, 1.25 and 2.49 mg L^{-1}	—	Deionized (DI) water	0.5 M $MgCl_2$	FO	11.4 L m^{-2} h^{-1}	—	3
							PRO	12.5 L m^{-2} h^{-1}		
		Polysulfone	0.01, 0.05 and 0.1 wt%	—	DI water	2 mol L^{-1} $MgCl_2$	FO	8 L m^{-2} h^{-1}	2 g m^{-2} h^{-1}	29
		Polyethersulfone	0.5, 1, 1.5, 2 and 2.5 wt%	—	DI water	1000 ppm NaCl	PRO	11.5 L m^{-2} h^{-1}	—	30
	GO	Poly L-lysine	0.08 mg cm^{-2}	—	Milli-Q water	2 M NaCl	FO	11 L m^{-2} h^{-1}	1.3 g m^{-2} h^{-1}	31
		Polydopamine	0.6 mg cm^{-2}	—	Milli-Q water	2 M NaCl	FO	13.63 L m^{-2} h^{-1}	0.68 mg min^{-1}	32
		Polysulfone	0.1, 0.25, 0.5 and 1.0 wt%	25 °C	DI water	0.5 M NaCl	FO	19.77 L m^{-2} h^{-1}	3.2 g m^{-2} h^{-1}	33
							PRO	41 L m^{-2} h^{-1}	6.3 g m^{-2} h^{-1}	
		Polyamide	0.1, 0.25, 0.5 and 1.0 wt%	25 ± 0.5 °C	DI water	2 M NaCl	FO	35.4 L m^{-2} h^{-1}	12.5 g m^{-2} h^{-1}	34
							PRO	56.6 L m^{-2} h^{-1}	14.5 g m^{-2} h^{-1}	
		Polyethersulfone	0.2, 0.5, 0.8 and 1.0 wt%	—	DI water	2 M NaCl	FO	41.4 L m^{-2} h^{-1}	170 mM m^{-2} h^{-1}	35
		Sulfonated polyethersulfone	0.1%	25 ± 1 °C	DI water	1 M Na_2SO_4	FO	25 L m^{-2} h^{-1}	1.5 g m^{-2} h^{-1}	36
							PRO	30 L m^{-2} h^{-1}	3 g m^{-2} h^{-1}	
	CNFs	Cellulose acetate/ cellulose triacetate	0.25, 0.5 and 1 wt%	25 °C	10 mM NaCl	Seawater	FO	15.6 L m^{-2} h^{-1}	0.4 g m^{-2} h^{-1}	37
Nano mineral materials	HNTs	Polysulfone	0.01, 0.05, 0.1 wt%	Room temperature	10 mM NaCl	2 M NaCl	FO	20.1 L m^{-2} h^{-1}	6.5 g m^{-2} h^{-1}	38
							PRO	34 L m^{-2} h^{-1}	8 g m^{-2} h^{-1}	
		Polysulfone	0.25, 0.5 and 1 wt%	25 °C	10 mM NaCl	2 M NaCl	FO	27.71 L m^{-2} h^{-1}	14.62 g m^{-2} h^{-1}	39
							PRO	43.25 L m^{-2} h^{-1}	27.52 g m^{-2} h^{-1}	
	Boehmite	Cellulose acetate/ cellulose triacetate	0.25, 0.5 and 1 wt%	—	10 mM NaCl		FO	23 L m^{-2} h^{-1}	6.5 g m^{-2} h^{-1}	1
							PRO	38.5 L m^{-2} h^{-1}	14.5 g m^{-2} h^{-1}	
	$CaCO_3$	Polysulfone	5, 7.5 and 10 wt%	Room temperature	DI water	2 M NaCl	FO	17 L m^{-2} h^{-1}	45 g m^{-2} h^{-1}	40
							PRO	27.6 L m^{-2} h^{-1}	50 g m^{-2} h^{-1}	
		Polyethersulfone	3,5 and 10 wt%	Room temperature	DI water	2 M NaCl	FO	52 L m^{-2} h^{-1}	16.8 g m^{-2} h^{-1}	41
							PRO	62 L m^{-2} h^{-1}	21.6 g m^{-2} h^{-1}	
	Silica	Polyacrylonitrile	0, 5, 10 and 15 wt/wt%	20 °C to 25 °C	DI water	1 M	FO	56 L m^{-2} h^{-1}	8 g m^{-2} h^{-1}	42
							PRO	74 L m^{-2} h^{-1}	11.8 g m^{-2} h^{-1}	
		Polysulfone	1, 3 and 5 wt%	25 ± 1 °C	DI water	2 M NaCl	FO	22.3 L m^{-2} h^{-1}	12 g m^{-2} h^{-1}	43
							PRO	41.9 L m^{-2} h^{-1}	19 g m^{-2} h^{-1}	
		Polysulfone	0.01, 0.05 and 0.1 wt%	30 °C	10 mM NaCl	2 M	FO	22 L m^{-2} h^{-1}	1.2 g m^{-2} h^{-1}	44
							PRO	36 L m^{-2} h^{-1}	1.5 g m^{-2} h^{-1}	
		Poly(vinylidene fluoride)	0.5, 1, 2 and 5 wt%	Room temperature	DI water	1 M	FO	52 L m^{-2} h^{-1}	34.84 g m^{-2} h^{-1}	45
	Zeolite	Polysulfone	0.02, 0.05, 0.1, 0.2 and 0.4 w/v%	20 ± 0.5 °C	10 mM	1 M	FO	14 L m^{-2} h^{-1}	3 g m^{-2} h^{-1}	21
							PRO	30.7 L m^{-2} h^{-1}	7 g m^{-2} h^{-1}	
		Polysulfone	0.5 and 1 wt%	20 ± 0.5 °C	DI water	2 M	FO	40 L m^{-2} h^{-1}	29 g m^{-2} h^{-1}	10
							PRO	86 L m^{-2} h^{-1}	58 g m^{-2} h^{-1}	

Table 2 (*Contd.*)

	Nanomodifier	Polymer	Component loading	Test temperature	FS	DS	Operating orientation	Water flux	Solute flux	Reference
Metal/metal-oxide nanoparticles	Ag	Polydopamine	0.22, 1.04, and 1.19%	Room temperature	Milli-Q water	0.5 M $MgCl_2$	FO	18 L m^{-2} h^{-1}	3.2 g m^{-2} h^{-1}	46
							PRO	42 L m^{-2} h^{-1}	3.4 g m^{-2} h^{-1}	
		Polydopamine	—	25.0 ± 0.5 °C	DI water	1 M NaCl	PRO	13.31 L m^{-2} h^{-1}	22.39 g m^{-2} h^{-1}	47
	TiO_2	Polysulfone	0.01, 0.05 and 0.1 w/v%	Room temperature	10 mM NaCl	2.0 M NaCl	FO	25.5 L m^{-2} h^{-1}	5 g m^{-2} h^{-1}	25
							PRO	40.8 L m^{-2} h^{-1}	7.5 g m^{-2} h^{-1}	
		Polysulfone	0.5 wt%	Ambient temperature	10 mM NaCl	2 M NaCl	FO	29.7 L m^{-2} h^{-1}	3.564 g m^{-2} h^{-1}	48
							PRO	56.2 L m^{-2} h^{-1}	13.488 g m^{-2} h^{-1}	
		Polysulfone	0, 0.3, 0.6 and 0.9 wt%	Ambient temperature	DI water	2 M NaCl	FO	33 L m^{-2} h^{-1}	15.7 g m^{-2} h^{-1}	4
							PRO	59.4 L m^{-2} h^{-1}	31 g m^{-2} h^{-1}	
		Polysulfone	0, 0.5, 0.75 and 1 wt%	Ambient temperature	10 mM NaCl	2 M NaCl	FO	29.7 L m^{-2} h^{-1}	7.3 g m^{-2} h^{-1}	14
							PRO	56.27 L m^{-2} h^{-1}	14.14 g m^{-2} h^{-1}	
		Polysulfone	0.01, 0.05 and 0.1 wt%	Ambient temperature	10 mM NaCl	0.5 M NaCl	FO	17.82 L m^{-2} h^{-1}	2.17 g m^{-2} h^{-1}	49

binders are employed to stiffen the structures of bucky-papers, the porosity is not greatly influenced.[74] Therefore, bucky-papers have drawn a great deal of attention[75,76] in the water separation[77] and purification[74] industries. The high compressibility[78] of bucky-papers restricts their use in reverse osmosis processes. Hence, researchers have turned their focus to FO due to the low pressures employed in this process. Dumée *et al.*[79] investigated a novel approach to interfacial polymerization on the surfaces of bucky-paper materials which were functionalized with hydroxyl groups. The fabricated super-porous bucky-paper membranes exhibited high hydrophilicity and excellent FO characteristics.

2.1.2 Graphene oxide. Two-dimensional GO nanosheets are a typical nanomaterial with extremely high specific surface area and atomic degree thickness.[80,81] Also, their surfaces contain abundant oxygen-containing functional groups, which can promote their interaction with polymers. Due to its unique structure and surface properties, GO is an ideal candidate for various applications.[27,82–85] Among these, membrane separation is a promising application to benefit from GO. Compared with other fillers, the extremely high aspect- and surface area-to-volume ratios of GO nanosheets promote better interactions with the polymer matrix. These unique dimensional and surface properties of GO nanosheets offer excellent potential for fabricating composite materials with excellent physical properties, flexible chemical functionalization, strong hydrophilicity and excellent antifouling properties.[80,86–88]

Studies using GO as a modifier to prepare nanofiltration and ultrafiltration hybrid nanocomposite membranes have achieved great improvements in hydrophilic and antifouling properties.[86,89–91] However, water desalination with GO-based membranes still faces challenges and remains controversial. Some researchers have reported that solute rejection of GO-based membranes or reduced GO-based membranes is weak in water desalination,[80,82,92–95] while other researchers have reported the opposite.[96,97] This argument has limited the research and large scale development of GO-based membranes. To overcome this dilemma, Sun *et al.*[98] studied and revealed the mechanism behind the controversy regarding GO-based membranes in water desalination. With the aid of isotope tracer labelling and molecular dynamics studies in water and ion diffusion, they showed the excellent potential of GO-based membranes in water desalination. Fig. 2 shows schematics of the mechanisms of water desalination and photographs of GO-based membranes with cross-sectional SEM images for concentration gradient-driven diffusion (Fig. 2(A)) and pressure-driven filtration (Fig. 2(B)). However, employing excess pressure will weaken the water–ion interactions with GO inter-lamination nanochannels and sequentially reduce the selectivity. Meanwhile, in concentration gradient-driven diffusion, GO-based membranes demonstrate intrinsic high water/ion selectivity, which confirms that GO is suitable for FO rather than pressure-driven filtration.

The potential of lamellar GO as a modification to improve the performance of FO membranes was also confirmed by Park *et al.*[33] They blended lamellar GO with polysulfone to obtain an organic–inorganic hybrid nanocomposite FO support layer.

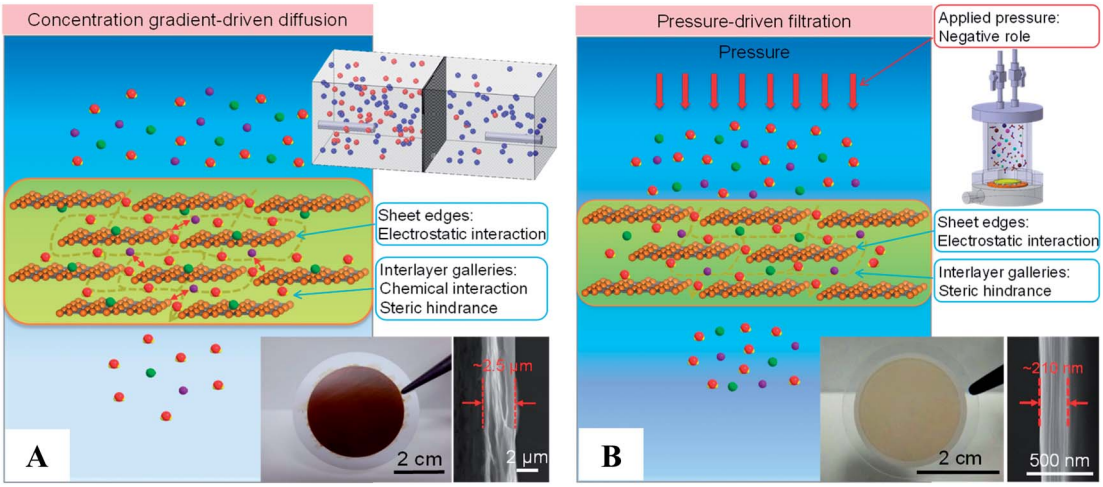

Fig. 2 (A) Schematic of the mechanism of water desalination, experimental setup, and photograph of a lamellar GO membrane on a microfilter with a cross-sectional SEM image for concentration gradient-driven diffusion. (B) Schematic of the mechanism of water desalination, experimental setup, and photograph of a lamellar GO membrane on a microfilter with a crosssectional SEM image for pressure-driven filtration.[98]

Subsequently, an FO membrane with high permeability and selectivity was obtained. Additionally, the lower structural parameter and higher hydrophilicity also enhanced the water permeability of the FO membrane. Later, a GO hybrid nanocomposite FO support layer was employed to improve the hydrophilicity and anti-fouling performance of a membrane. However, GO could not provide its full benefits when it was buried inside the polymeric matrix. To take advantage of the excellent properties of GO, Shen *et al.*[34] incorporated GO nanosheets with a polyamide active layer to fabricate a hybrid nanocomposite membrane for the FO process. This method utilized very little GO while attaining excellent performance, including high separation performance and water flux and decreased fouling propensity, by simply embedding a small quantity of GO into the support layer.

Maintaining the stability of a GO hybrid nanocomposite membrane is also necessary in water purification treatment. Simple blending or coating methods to fabricate GO hybrid nanocomposite membranes carry the risk of diffusing hydrophilic lamellar GO into the hydrosphere, which can be absorbed by aquatic creatures and thereby affect human beings. Hence, researchers have made efforts to prepare GO lamellae that are strongly bound to each other and the membrane to mitigate this risk. Hanaa *et al.*[31] attached GO to the active layers of FO membranes through a poly L-lysine intermediary by both layer-by-layer (LbL) and hybrid grafting methods. The resulting hybrid FO membranes exhibited excellent antifouling properties. These membranes killed 99% of bacteria and showed reduced permeability compared to the original membrane. For the same purpose, Hegab *et al.*[32] employed the bioadhesive polydopamine to immobilize GO onto the surface of FO membranes *via* self-assembly and oxidative polymerization methods. The fabricated membrane simultaneously possessed high permeability, high rejection and excellent antibiofouling properties.

Graphitic carbon nitride, which has a similar two-dimensional laminated structure to graphene, is a derivative of GO. It possesses excellent optical and chemical properties as well as good catalytic activity[99] and thermal stability and has attracted increasing attention. Graphitic carbon nitride is a cellular structure with a plentiful curved lamellar morphology.[100] It can enhance the hydrophilicity of membranes because its nitrogen atoms can form hydrogen bonds with water molecules. Wang *et al.*[35] prepared graphitic carbon nitride as a modifier for a porous polyethersulfone support layer of FO membranes. The results revealed that a lower structural parameter and ICP were obtained, which suggests that graphitic carbon nitride is an effective modifier to enhance FO membrane performance.

2.1.3 Carbon nanofibers (CNFs). CNFs consist of rolled multilayer graphite sheets with diameters in the range of 10 nm to 500 nm. Due to their excellent chemical activity and electroconductivity, high tensile moduli and strength, they are useful in many fields. CNFs are a quasi-one-dimensional carbon material with similarities to both CNTs and ordinary carbon fibers. Unlike CNTs or other carbon nanostructures, which have low dispersion and chemical inertness, the sidewalls of CNFs have higher chemical activity and can be readily chemically functionalized with more options. The edges of CNFs are exposed and their edge sites are active, which is beneficial to the chemical functionalization of the surface of CNFs to improve their dispersibility in casting solutions. Due to their high dispersibility in polymeric matrices, CNFs are considered to be a candidate for employment in the fabrication of high-performance membranes. Zoheir Dabaghian *et al.*[37] synthesized a cellulose triacetate FO membrane incorporated with carboxylated CNFs *via* a phase inversion method. The modified membrane exhibited high water flux and low solute permeation. Tensile strength measurements confirmed that this parameter of the modified FO membrane was much higher than that of unmodified cellulose triacetate.

2.2 Nanomineral materials

Nanomineral materials, including montmorillonite, halloysite, and zeolites, are nanomaterials with enormous surface areas

and porous structures. Nanomineral materials have numerous advantageous properties, such as porosity, good adsorption performance, stability, wide availability of raw materials, low cost, large specific surface area, good adsorption performance, light weight and lack of secondary pollution. Due to their unique structures and excellent properties, nanominerals are suitable for water purification. Studies revealed that the addition of nanomineral materials improves the water permeability and solute rejection of membranes, while the increased number of hydrophilic groups improves their anti-pollution properties. Dispersion of nanomineral materials is key to the preparation of thin film nanocomposite membranes. Sufficient dispersion in the membrane increases its pore size uniformity, porosity, and water flux. Moreover, nanomineral loading can result in high porosity and ideal hydrophilicity of membranes that mitigate the negative effects of ICP, which generally influences FO processes.

2.2.1 Halloysite nanotubes (HNTs). Alumina-silicates (also called HNTs) are nanominerals that can be obtained from natural origins and possess excellent biocompatibility. According to electric effects, HNTs exhibit dual charge functionality. Containing numerous siloxane groups, the ektexine of HNTs is negatively charged, while the endosexine is rich in hydroxyl groups and positively charged.[101] Moreover, the tubular structure and low content of hydroxyl groups on the surface of HNTs endow them with good consistency in polymeric matrices.[102] Due to these interesting properties, HNTs are promising modifiers in membrane separation processes.[103] The influences of HNT incorporation on the filtration performance of FO membranes include hydrophilicity, porosity, roughness, water flux and the structural parameter. Although their structure is similar to that of CNTs, HNTs possess a unique dual charge functionality and significantly lower cost.[104]

With the aim of improving membrane performance, Ghanbari *et al.*[38] incorporated various concentrations of HNTs into the active layer of FO membranes by *in situ* interfacial polymerization. The results indicated that the water flux, rejection and antifouling properties of all the fabricated hybrid nanocomposite FO membranes were better than those of the pure polymeric membrane. Subsequently, the group blended HNTs into a polysulfone support layer to study the influence of HNTs on ICP behavior.[39] The results showed that the incorporation of HNTs in the support layer can reduce the structural parameter and mitigate ICP.

2.2.2 Boehmite. Boehmite nanoparticles, which have the chemical composition AlOOH, contain abundant hydroxyl groups on their surfaces. Studies have revealed that due to their porous and hydrophilic structure, incorporating boehmite nanoparticles can enhance the performance of membranes, such as their water flux, structural parameter and separation performance.[1,105,106] It was proved that 0.5 wt% capacity of boehmite nanoparticles could result in a threefold increment of water permeability and a decreased structural parameter of 0.53 mm without sacrificing solution rejection compared with the original pure membrane.[1]

Zirehpour *et al.*[1]employed boehmite to modify cellulose triacetate FO membranes. A strong interaction formed due to hydrogenic reactions between the hydroxyl groups in boehmite and cellulose triacetate, which enhanced the compatibility between the polymeric matrix and boehmite nanoparticles. Hence, the fabricated membrane gave rise to more effective water flux.

2.2.3 Silica. Silica as an inorganic additive to prepare hybrid nanocomposite membranes has a wide range of applications due to its mild reactivity, thermal resistance, convenient operation, mechanical strength, small size, nontoxic nature, strong surface energy, good suspendability in aqueous solution and environmental friendliness.[107–110] Researchers testified that the incorporation of silica nanoparticles afforded polymeric membranes with enhanced mechanical strength[111–116] and thermal stability.[117–120] In addition, silica nanoparticles have an impact on the polymerization reactions of the polymeric matrix.[121] This property is due to the strong interactions at the interface between the silica and the polymeric matrix[121] which is formed by the immobilized amorphous layer of polymer molecules on the silica nanoparticles. Because silica nanoparticles are smaller in size, they have better dispersion performance in solution. Silica/polyamide reverse osmosis membranes have higher water flux and rejection compared with unmodified reverse osmosis membranes,[44] which provides a good choice for FO applications. Niksefat *et al.*[44] fabricated polyamide nanocomposite FO membranes containing silica nanoparticles *via in situ* interfacial polymerization. The fabricated nanocomposite membrane exhibited greatly enhanced water permeability and solute rejection compared to the original membrane with silica loading concentrations between 0.01 and 0.1 wt%.

Novel amorphous silica nanoparticle-incorporated poly(vinylidine fluoride) electrospun nanofiber mats were fabricated by Obaid *et al.*[45] as support layers for FO membranes. The results showed that the membrane showed high salt rejection and water flux. Moreover, this formulation displayed the lowest structural parameter ($S = 29.7$ μm), which represents approximately 69% reduction compared to the pristine membrane. Electrospinning is an excellent technology to produce nanofiber films with advantages such as low tortuosity, high porosity, and low thickness. The nanofiber-composed scaffold structure is an ideal candidate as a support layer in FO processes; it has remarkable advantages in comparison to conventional sponge-like or finger-like pore structures. Nanofiber films as support layers possess unique advantages, including internally connected channels for salt and water transportation. This property can provide an excellent environment to mitigate ICP.[122]

2.2.4 Zeolite. Zeolite was the first nanomaterial to be induced into FO membranes. Before that, zeolite was frequently used as a modifier in polymeric membranes for gas separation or pervaporation due to its uniform pore size distribution, channel structures and abundant negatively charged sites. The unique sub-nanometer pores of zeolites provide shape selectivity, which improves the adsorption efficiency of gas molecules.[123] Zeolite is composed of aluminosilicates, which provide negatively charged defect sites to neutralize the positive charges of protons and ultimately form Brønsted acid sites.[124] These unique characteristics have drawn the attention of researchers and demonstrate the enormous potential of zeolite in

separation processes. Some types of zeolite, such as NaA, are deemed to have the highest hydrophilicities among inorganic nanomaterials. They are so stable in most aqueous and organic solvents that it is difficult to break them off from the polymeric matrix.[125] It has been testified that blending zeolite in the polyamide active layer of reverse osmosis membranes[126–129] can enhance water flux without sacrificing solute rejection due to the presence of abundant sub-nanometer pores which play the role of preferential flow channels. In the separation process, water molecules pass through these tiny sub-nanometer pores, which are too small for solutes to cross.[21] Therefore, incorporation of zeolite in polymeric FO membranes was demonstrated to improve their water permeability without significant loss of salt rejection. Although zeolite hybrid nanocomposite membranes were originally produced for gas separation and reverse osmosis processes, their substantially increased water flux also suggests their usefulness in FO. Furthermore, blending zeolite into the support layer results in enhanced porosity and mitigates the ICP effect in FO processes. Ma *et al.* blended NaY zeolite into the polyamide active layer; the resulting FO membrane exhibited higher water permeability, possibly because of the porous structure of zeolite.[21] Subsequently, they incorporated zeolite nanoparticles into the support layer of FO membranes and fabricated a polysulfone hybrid nanocomposite matrix which exhibited higher porosity and hydrophilicity. The resulting membrane also showed significantly enhanced water permeability and a decreased substrate structural parameter compared to the original polysulfone support membrane.[10]

2.2.5 Nano-$CaCO_3$. $CaCO_3$ nanoparticles are among the most widespread, industrialized and inexpensive nanomaterials. The mature production technology of $CaCO_3$ nanoparticles is due to their surface polarity and their readily tunable particle size in production processes.[130] Thus, it is possible for $CaCO_3$ nanoparticles to meet the heavy demand of large scale production of polymeric membranes and play the role of sacrificial components. Wu *et al.*[40] blended $CaCO_3$ nanoparticles into a polysulfone substrate and then dissolved it with hydrochloric acid to increase the porosity of the support layer. The higher porosity of the fabricated FO membrane led to a smaller structural parameter and, thus, decreased ICP, which is advantageous to enhance water permeability and reduce mass transfer resistance.

Moreover, $CaCO_3$ is a good biomineral which also has high hydrophilicity due to its ionic bonds and hydrogen bonds with water molecules. Inspired by bio-mineralization processes in nature and the intrinsic hydrophilicity of minerals, inorganic mineral coating is an alternative method to impart hydrophilicity to a support layer without sacrificing other functional properties. Biomineralization can form a stable organic–inorganic hybrid structure by the interactions between certain organic and inorganic ions. Qing *et al.*[41] coated $CaCO_3$ continuously and uniformly throughout a polyethersulfone support layer. Resulting from the intrinsic hydrophilicity of the $CaCO_3$ coating, the hydrophilicity of the support layer was significantly increased and the structural parameter of the membrane was reduced to a similar value to those of cellulose-based membranes, with unchanged mechanical strength.

2.3 Metal/metal-oxide nanoparticles

For decades, metal nanoparticles and metal oxide nanoparticles have been widely used to address various environmental issues, especially in water desalination and regeneration.[131–133] Metal nanoparticles and metal oxide nanoparticles are known to be environmentally friendly, stable to UV irradiation, antibacterial and highly hydrophilic.[134] Due to the higher affinity of metal oxides to water, membranes incorporating metal and metal oxide nanoparticles are more hydrophilic than pure polymeric membranes.[135] Additionally, some metal oxide nanoparticles have accessible reactive anchoring sites, such as hydroxyl and silanol groups, for further surface reactions to facilitate interactions with the polymer host matrix.[136] Also, some metal and metal-oxide nanoparticles have unique properties, such as antibacterial properties and photochemical catalysis, which aid FO membrane processes.

2.3.1 Ag nanoparticles. Ag nanoparticles have the most comprehensive antibacterial spectrum; they are effective against various aquatic microorganisms, such as bacteria, fungi, and algae.[137] Ag nanoparticles can destroy the cytomembrane and impede the metabolism of microorganisms by releasing dissolved Ag or producing active oxygen.[138] Introducing Ag nanoparticles into membranes to filter water rich in microorganisms has been suggested as a method to alleviate the biological contamination resulting from blooms of microorganisms, resulting in innocuous and pollution-free water sources.[139–141] The antibiofouling properties of Ag nanoparticles are durable. Their dissolving and releasing behaviors can be well tuned compared to those of Ag ions. Hence, Ag nanoparticles have gained increasing focus for their excellent antibiofouling properties.[142] Ag nanoparticles have been incorporated into microfiltration,[138,143] ultrafiltration,[144,145] nanofiltration[146] and reverse osmosis[147] membranes by different methods, such as surface modification, blending and *in situ* interfacial polymerization. Subsequently, Liu *et al.*[148] fabricated Ag hybrid nanocomposite nanofiltration and FO membranes by an LbL assembly method. The assembly of Ag nanoparticles in the membranes did not produce negative effects on the fabricated membrane. Also, even at a low concentration of Ag nanoparticles, the membrane performance in separation processes was significantly enhanced. Furthermore, the antibiofouling properties of the resulting Ag nanocomposite membranes were also greatly improved against both Gram-positive *Bacillus subtilis* and Gram-negative *Escherichia coli*.

2.3.2 TiO_2 nanoparticles. TiO_2 nanoparticles are one of the most promising metal oxide nanoparticles due to their high hydrophilicity and excellent photocatalytic properties with perfect mechanisms.[149,150] As an acknowledged photocatalytic material, TiO_2 has been extensively used in disinfection and decomposition applications; these characteristics also make TiO_2 a promising anti-fouling modifier.[25,151] Moreover, due to the chemical stability, controllable morphology, surface properties, photocatalytic function and antifouling performance of TiO_2 nanoparticles, they are useful in membrane processes.[152–156] Numerous studies regarding the introduction of TiO_2 nanoparticles into

membranes have confirmed its viability and effectiveness, leading not only to enhanced hydrophilicity and water permeability, but also to sterilization and antibiofouling abilities.[151,157,158] The inherent photocatalytic properties of TiO_2 aid in enhancing the antifouling performance of membranes[159] by disintegrating macromolecular contaminants. Amini's group[4] introduced TiO_2 nanoparticles into a polysulfone support layer to reduce the structural parameter and alleviate the ICP of FO membranes. The resulting support layer exhibited both high hydrophilicity and porosity with the presence of TiO_2 nanoparticles.

However, the performance of hybrid nanocomposite membranes is restricted by nanoparticle agglomeration. Studies have been performed to enhance the consistency of TiO_2 nanoparticles in the polymeric matrix and produce a uniform surface. Maryam Amini *et al.*[160] used a silicane coupling agent to achieve chemical modification of TiO_2 and incorporated it into a polyamide active layer by *in situ* interfacial polymerization. The results indicated that the introduction of modified TiO_2 significantly changed the surface properties of FO membranes and mitigated the agglomeration behavior. The hybrid nanocomposite FO membranes showed high water flux and stable rejection rates at all TiO_2 loading concentrations compared with the original membrane.

3. Effects of modification methods on FO membrane performance

In recent years, with the development of membrane separation techniques in water treatment and other fields, the requirements of membrane function, such as permeability, selectivity, anti-pollution, chemical and thermal stability, are becoming increasingly strict. Traditional membrane fabrication methods have difficulty meeting these application requirements. Therefore, researchers have begun to turn their focus to developing new composite membranes and modification methods to obtain satisfactory properties. Membrane modification is considered to be an effective method to improve the comprehensive performance of membranes. The modification methods can be divided into chemical modification and physical modification. Chemical modification methods include LbL assembly, grafting, and hydrolysis. Physical modification methods include blending methods, surface coating, and *in situ* interfacial polymerization. In this section, four main methods, including blending, *in situ* interfacial polymerization, surface grafting and LbL assembly, are listed and analyzed. Fig. 3 provides a schematic of these modification methods of nanocomposite membranes.

3.1 Blending

Blending is a simple and common method to prepare hybrid membranes that can be used with a large range of materials; it is one of the most important methods to modify polymeric membranes. The introduction of nanomaterials enhances the mechanical strength of membranes and prevents collapse and structure destruction of the porous support layer. The blending membranes are typically obtained by mixing an inorganic dispersed phase in a continuous polymeric matrix. Blending nanomaterials such as TiO_2 nanoparticles,[4,14] CNTs,[30] porous zeolite nanoparticles[10] and GO nanosheets[35] into the support layer of FO membranes has been attempted, and the resulting membranes exhibited brilliant performance. Especially, these nanomaterials enhance the physical and structural characteristics of the support layer, which leads to increased hydrophilicity and/or porosity.[33]

Blending nanomaterials can significantly enhance membrane performance, such as water flux, rejection, stability, antifouling, and catalytic activity, in FO membrane separation processes;[161–163] meanwhile, the adverse impact of ICP is mitigated.[164] The size, dispersity, morphology and compatibility of the nanomaterials affect the performance of the fabricated membrane. Preparing membranes by blending is a simple process which is easy to operate, and the concentration of the components can be readily controlled. However, the inorganic components, especially nanoparticles, can readily aggregate. For the purpose of preventing inorganic nanomaterials from agglomerating and enhancing the consistency between the organic and inorganic phases, it is significant to modify the inorganic nanomaterials so as to obtain stronger interactions with the polymeric matrix. Additionally, incorporation of a solubilizing agent or crosslinking agent can enhance the consistency and modify the defects of the hybrid nanocomposite membranes. GO,[33] CNTs,[3,30] TiO_2,[4,14,48] zeolite,[10] silica,[10] and many other nanomaterials have been used in blending methods to synthesize FO membranes. Studies confirmed that blending nanomaterials into the support layers of FO membranes can effectively enhance water flux without reducing rejection, which results from the higher hydrophilicity and porosity conferred by the nanoadditive. In addition, the polymer layer can also benefit from the physical mechanics, magnetism, optics and conductivity, and catalytic and biomedical properties of doped inorganic nanoparticles.

3.2 *In situ* interfacial polymerization

In situ interfacial polymerization is defined as uniformly mixing inorganic particles with organic monomers and inducing monomer polymerization under appropriate conditions.[156] The fabricated ultrathin film serves as the active layer of an asymmetric membrane. *In situ* interfacial polymerization methods include suspension polymerization, dispersion polymerization, emulsion polymerization and polymerization between the functional groups on the inorganic particles and the monomer so as to immobilize the polymer phase network structure as a chemical bond. *In situ* interfacial polymerization is convenient to operate; however, it does have challenges, such as facile agglomeration of the inorganic nanoparticles and uneven dispersion. Studies have confirmed that hybrid active layers fabricated by introducing nanomaterials in a monomer solution significantly improve membrane performance, such as water flux, solute rejection, catalytic activity, specific area, antifouling and thermal stability in membrane separation

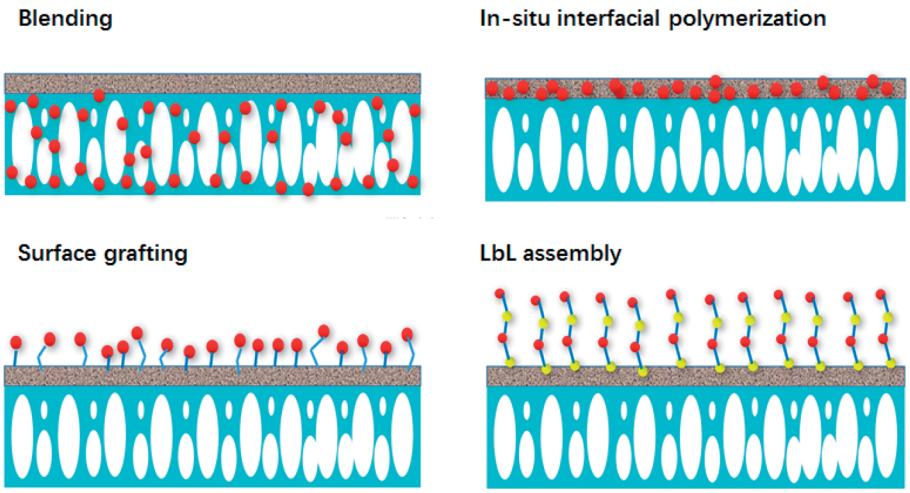

Fig. 3 Schematic of various modification methods of nanocomposite membranes.

processes. To date, hybrid nanocomposite FO membranes fabricated by *in situ* interfacial polymerization methods have been developed by introducing TiO_2,[25,165] titanate nanotubes,[49] MWCNTs,[8] HNTs,[38] silica,[44] GO[31,33] and zeolite[21] into the polyamide active layer. This corresponds to the concept of nanocomposite membranes that incorporate nanomaterials into the active layers of conventional pure polymeric membranes.[127]

A conflict in FO separation processes is that solute rejection cannot increase simultaneously with water flux; this is called the trade-off effect. That is to say, a membrane with high water permeability usually has low rejection. Therefore, preparing FO membranes with both high flux and high solute rejection is a great challenge. Introducing inorganic nanomaterials in polyamide active layers *via in situ* interfacial polymerization is an effective solution of the trade-off effect which can not only improve the hydrophilicity, but can also impart antifouling properties to a membrane. The inorganic nanoparticles doped in the polyamide layer can increase the water flux of the membrane by providing water channels directly or by changing the network structure of the membrane. Therefore, the doping of porous inorganic nanomaterials into polyamide active layers has received focus to improve the separation performance of membranes.

3.3 Surface grafting

Surface grafting involves introducing inorganic nanoparticles or organic functional groups onto the surface of membranes through various methods, such as photoinitiation and induction by radiation. Free radical active sites are produced on the polymeric molecular chain of the membrane surface through a series of pretreatments, and the radical ion is then polymerized with the modified monomer. Analogous methods to introduce inorganic nanomaterials into polymeric membranes, such as blending and depositing, face a common problem: the binding forces between the nanomaterials and the polymeric membrane are so weak that the nanomaterials can be readily separated from the membrane. Connecting inorganic nanomaterials with the polymeric membrane by chemical bonds, such as surface grafting, is a good solution to enhance the immobility of hybrid nanocomposite membranes.[166] This suggests that surface grafting is an ideal method to fabricate immobile and durable hybrid nanocomposite membranes. Zhong *et al.*[167] fabricated nanofiltration membranes using sponge-like sulfonated polyphenylenesulfone support layers with positive charge *via* a UV-initiated grafting method. However, only photosensitive polymers can be used as support layer materials for UV grafting, which impedes the development of this method. Hegab *et al.*[31] prepared hybrid nanocomposite FO membranes by surface grafting to introduce GO on the surface of a polyamide active layer.

3.4 Layer-by-layer (LbL) assembly

LbL assembly is used to alternately form oppositely charged polyelectrolyte thin films on a matrix which are connected by electrostatic absorption and van der Waals forces.[36,168] LbL assembly has received focus because it is a convenient and versatile method to form active layers for high-performance nanofiltration,[169,170] reverse osmosis and FO membranes.[171,172] LbL is a highly versatile membrane preparation technology with good thermal stability, high solvent resistance, low operating expense, *etc.*[173–175] Nanomaterials can be introduced into the layered structure of LbL assembly membranes flexibly with tunable loading components and structures. LbL assembly show great potential in industries such as water treatment and food processing.[5,176] Employing LbL assembly, Liu *et al.*[148] prepared Ag hybrid nanocomposite FO membranes. They assembled Ag nanoparticles on the surfaces of the FO membranes; at low loading concentrations of Ag nanoparticles, there was no negative impact on the membrane performance. The separation performance of the fabricated LbL assembly hybrid nanocomposite membranes was no less than those of most nanofiltration-like FO membranes. Furthermore, the Ag hybrid nanocomposite FO membranes demonstrated brilliant antibiofouling characteristics against both Gram-positive

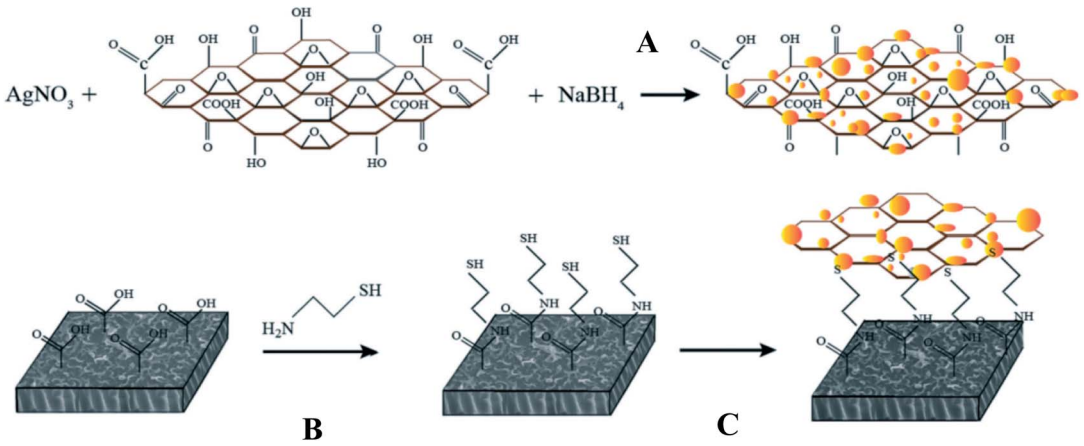

Fig. 4 Covalently bonded AgNP-decorated GO nanosheets through click chemistry on FO membranes: (A) *in situ* Ag nanoparticles synthesized onto the GO nanosheets, (B) amide forming reaction and thiol functionalization of the FO membrane, and (C) covalent bonding of the GO/Ag nanocomposites to the FO membrane surface.[181]

Bacillus subtilis and Gram-negative *Escherichia coli*. Hegab *et al.*[32] prepared polydopamine/GO composites and introduced them onto the support layers of FO membranes *via* LbL assembly. The polydopamine played the role of reducing GO and bonding it onto the membrane surface *via* self-assembly and oxidative polymerization. The fabricated membrane possessed enhanced water flux and solute rejection as well as excellent antibiofouling performance.

4. Discussion and outlook

With the continuing development and progress in nanotechnology, novel methods have inspired the design and production of multifunctional hybrid nanocomposite FO membranes.[177] Introducing inorganic nanomaterials can result not only in excellent separation performance but also in new functions that are inherited from the inorganic nanomaterials. Brand new insight has been provided to create the next generation of high performance FO membranes with antifouling properties, low ICP and decreased trade-off effects. Organic–inorganic hybrid nanocomposite FO membranes, in contrast with conventional polymeric membranes, are confirmed to have great promise to overcome the bottleneck of ICP. However, the applications of these nanocomposite FO membranes have yet to expand beyond the laboratory. Despite a series of excellent enhancements in performance, successful practical applications and commercialization are rare. Some challenges still exist for the large scale industrial application of FO membranes, including creating suitable draw solutes and building integrated sustainable FO systems. Draw solution is one of the key factors of FO processes which distinguishes FO from other pressure-driven membrane techniques. An ideal draw solution must furnish a high osmotic gradient and possess efficient recovery with low energy consumption. Furthermore, a system for water purification and draw solution reuse is also necessary. One example is an FO–ultrafiltration (FO–UF) series for desalination with an FO membrane as the main component for salt rejection and a UF membrane as a post processing method for regeneration of the draw solution.[178] It has been suggested that more research should be focused on integrated FO systems, as they may be an important factor in the large scale industrial application of FO in the future.[179,180]

Regarding hybrid nanocomposite FO membranes, the main challenges include the agglomeration of nanomaterials, low filtration efficiency caused by ICP, and the high cost of nanomaterials. The commercialization of nanocomposite membranes for water treatment is still in its infancy. Therefore, more studies on organic–inorganic hybrid nanocomposite FO membranes are needed to achieve better performance and overcome the barriers that limit FO. This section discusses the challenges facing the practical application of nanocomposite FO and some advanced nanotechnology in the membrane field that is beneficial to FO.

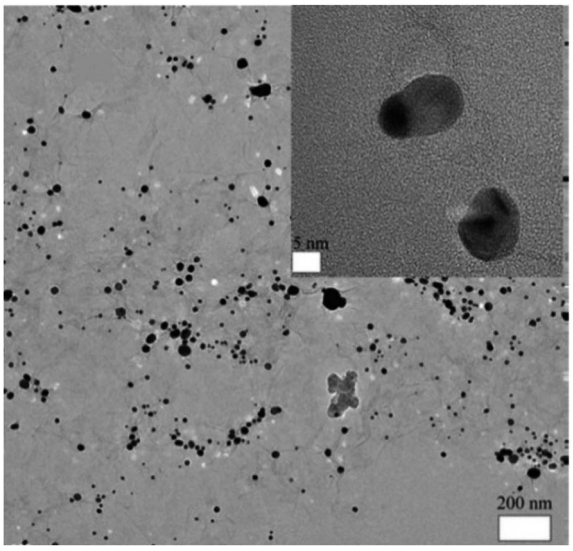

Fig. 5 High resolution transmission electron microscopy (HR-TEM) images of the GO/Ag nanocomposite.[181]

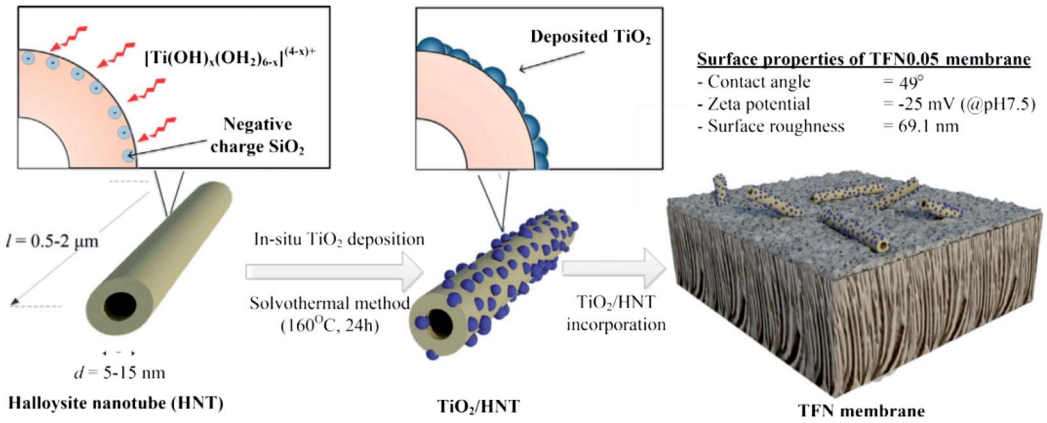

Fig. 6 Schematic of TiO_2 loading on the surface of HNTs.[165]

First, agglomeration is one of the main obstacles to introducing nanoparticles in polymeric membranes; it leads not only to uneven distribution in the membrane but also to decreased separation abilities by changing membrane structures, such as surface morphology and porosity. Aggregation is a common phenomenon that occurs during the preparation of hybrid nanocomposite membranes and impedes the homogeneous dispersion of nanomaterials in the polymeric matrix. Many efforts have been made to alleviate this phenomenon, among which surface modification of nanomaterials and optimizing the fabrication conditions are conventional methods that have achieved improved dispersion of nanomaterials.

In addition to surface modification and technology optimization, multi-component composite nanomaterials[182] have become increasingly popular in membrane preparation due to the various options and multiform characteristics provided by different nanomaterial combinations. For example, GO nanosheets were employed to stabilize Ag nanoparticles and enhance the contact between Ag and bacteria.[181] Ag nanoparticles were dispersed uniformly on the surface of GO nanosheets as an FO membrane modifier to prevent their agglomeration. Fig. 4 shows a schematic of the synthesis route of Ag-decorated GO nanosheets, and HR-TEM images of the fabricated nanosheet are shown in Fig. 5. Similarly, Ghanbari *et al.*[165] fabricated a TiO_2/HNTs composite nanomaterial *via* a one-step solvothermal method as an additive for FO membranes. Regarding filtration performance, the hybrid nanocomposite membrane showed excellent water flux and solute rejection. Due to the hollow tubiform structure of HNTs and the addition of antifouling and photochemical catalysis abilities from TiO_2, TiO_2/HNTs is a beneficial modifier. These composite nanomaterials are promising in improving the antifouling behavior of polymeric FO membranes for organic pollution separation. Fig. 6 illustrates the TiO_2 loading on the surface of the HNTs, and Fig. 7 shows transmission electron microscopy (TEM) images of TiO_2/HNTs with different scale bars.

Second, some nanomaterials can provide effective water transformation channels, such as CNTs. Recent computer simulation studies have indicated the high selectivity and water flux of CNTs; thus, they are ideal candidates for adsorption and separation applications.[183,184] However, blending a small quantity of CNTs and similar nanomaterials cannot ensure that water molecules are induced to move only through the nanotubes. In order to make full use of the water transport channels of CNTs, for the first time in 2004, researchers incorporated an array of aligned CNTs across a polymer matrix vertically and

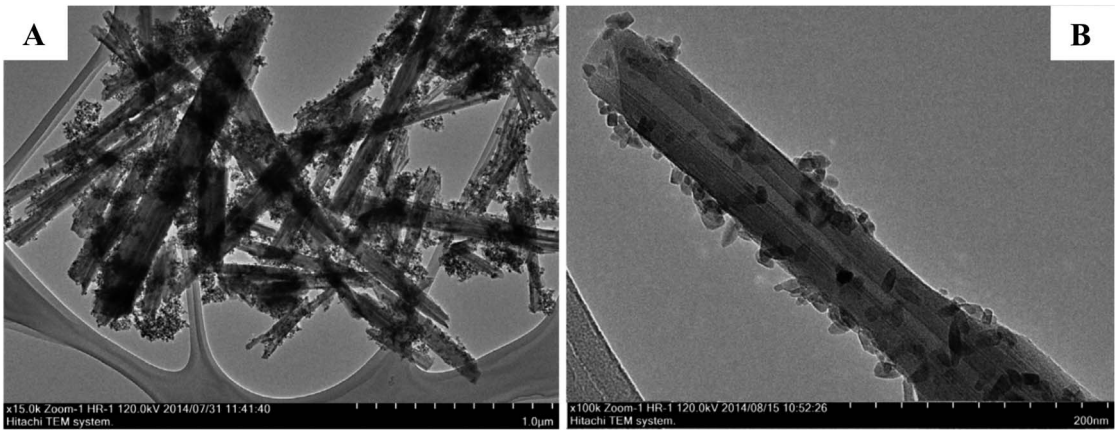

Fig. 7 TEM images of TiO_2/HNTs with different scale bars: (A) 1000 nm and (B) 200 nm.[165]

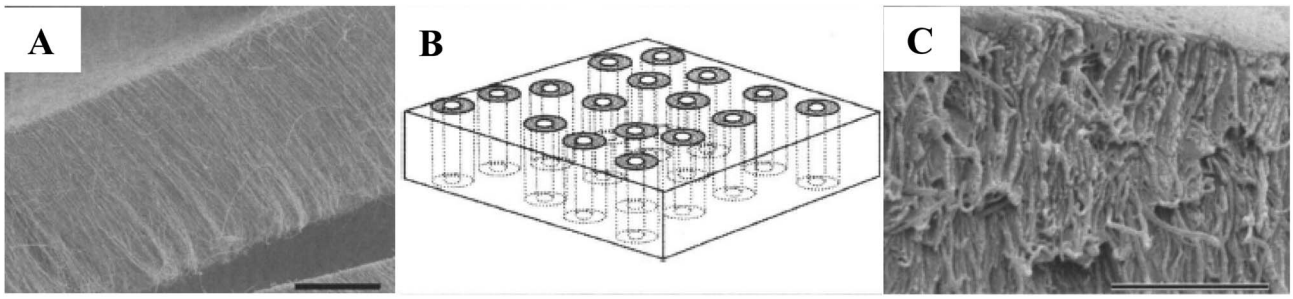

Fig. 8 (A) An as-grown, dense MWCNTs array produced with an Fe-catalyzed chemical vapor deposition process. Scale bar, 50 μm. (B) Schematic of the target membrane structure. With a polymer embedded between the CNTs, a viable membrane structure can be readily produced, with the pore being the rigid inner-tube diameter of the CNT. (C) The cleaved edge of the CNT-PS membrane after exposure to H_2O plasma oxidation. The PS matrix is slightly removed to contrast the alignment of the CNTs across the membrane. Scale bar, 2.5 μm.[185]

compactly to form a well-organized nanoporous membrane structure.[185] Fig. 8(A) shows a SEM micrograph of the as-grown MWCNTs. In Fig. 8(B), the ideal membrane structure diagram is presented. The lacunes between the CNTs are padded with a continuous polymer matrix, and the generally closed ends of the CNTs are etched open. Fig. 8(C) reveals the cleaved edge of the freestanding CNT membrane. After that, researchers began studying the mechanism of liquid transport through nano-sized channels. It was found that in the cavities of CNTs, the quantity of liquid transport was 1000 times greater than predicted. A microgeometry theory was proposed regarding the use of aligned CNTs[186] for water treatment,[187] and an approach to establishing an impeccable membrane system was provided.[188] Among the studies on CNT-based nanocomposite membranes in the water treatment field, the aligned CNTs matrix is believed to be a potential candidate as a support layer of FO membranes. Its superpermeable property has great promise in increasing the water flux of FO membranes as well as decreasing ICP.

Third, blending modification and surface modification are two main methods to introduce inorganic nanoparticles into organic polymer membranes.[189,190] However, nanomaterials cannot be strongly anchored on the surface of the membranes by surface modifications such as coating. The nanomaterials may be lost in the filtration process, which not only affects the membrane performance, but can also readily cause secondary water pollution. Although blending nanomaterials with casting solution can mitigate the loss of nanomaterials, there is an inherent dilemma that most nanomaterials are embedded within the polymeric matrix when the film is formed. This phenomenon decreases the modification efficiency severely, and the advantage of the nanomaterial surface structure cannot be fully exploited. Based on the above problems, our group[191] proposed a "blending-migration induced by a magnetic field" route to prepare nanocomposite membranes. We induced migration of magnetic nanomaterials to the top surface of the film using a magnetic field and fabricated an ultrafiltration membrane with hydrophilicity as well as antimicrobial and autocatalytic performance. Herein, a Fe_3O_4/GO–poly(vinylidene fluoride) hybrid ultrafiltration membrane was fabricated *via* a combination of magnetic field-induced casting and a phase inversion technique. Fe_3O_4/GO nanocomposites migrated toward the top surface of the membrane due to magnetic attraction and thereby rendered the surface highly hydrophilic, with robust resistance to fouling. Fig. 9 illustrates the main mechanism of GO migration under a magnetic field. Fig. 9(A) shows the procedure of the migration, while Fig. 9(B) shows the final results with/without a magnetic field. This technique is promising and useful for the preparation of support layers of FO membranes. The gradient distribution of nanomaterials in the polymeric matrix can enhance the utilization ratio of the nanomaterials and mitigate ICP effectively.

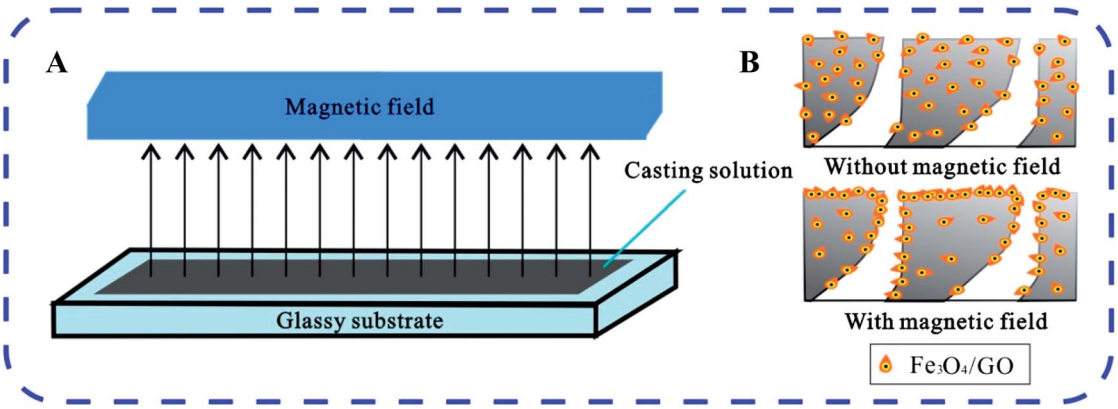

Fig. 9 Schematic of the mechanism of GO migration under a magnetic field.[191]

Finally, some negative critiques indicate that the nanomaterials commonly used in membrane preparation have high intrinsic cost, such as TiO_2, Ag nanoparticles, and GO, related to their raw materials and preparation technologies. To date, there have been numerous laboratory-scale studies on organic–inorganic hybrid nanocomposite FO membranes. However, due to their cost and some other factors, very little large scale production or industrial application has been practiced. Therefore, developing low-cost nanomaterials and cost-effective FO membranes with execellent performance is a future goal. Cost-effective large scale membrane fabrication includes the supplies of nanomaterials, additional procedures for nanomaterial incorporation, and monitoring of the long-term stability of membranes under practical application conditions. The less expensive ZnO, $CaCO_3$,[40,41] HNTs,[38,39] zeolite,[10,21] *etc.* are seemingly more economically feasible substitutes. More studies are still needed to reduce the expense of nanomaterials and identify new nanomaterials with lower production costs.

Conflicts of interest

There are no conflicts to declare.

Acknowledgements

The work was funded by the National Natural Science Foundation of China (11575126), the Qaidam Salt Chemical Joint Fund of National Natural Science Foundation of China – People's Government of Qinghai Province (U1607117), the Natural Science Foundation of Tianjin (16JCZDJC36400) and the Science and Technology Plans of Tianjin (15PTSYJC00230).

References

1 A. Zirehpour, A. Rahimpour, F. Seyedpour and M. Jahanshahi, *Desalination*, 2015, **371**, 46–57.
2 P. Lu, S. Liang, T. Zhou, X. Mei, Y. Zhang, C. Zhang, A. Umar and Q. Wang, *RSC Adv.*, 2016, 6.
3 K. Goh, L. Setiawan, L. Wei, W. Jiang, R. Wang and Y. Chen, *J. Membr. Sci.*, 2013, **446**, 244–254.
4 D. Emadzadeh, W. J. Lau, T. Matsuura, A. F. Ismail and M. Rahbari-Sisakht, *J. Membr. Sci.*, 2014, **449**, 74–85.
5 T. Cath, A. Childress and M. Elimelech, *J. Membr. Sci.*, 2006, **281**, 70–87.
6 M. Obaid, H. O. Mohamed, A. S. Yasin, O. A. Fadali, K. A. Khalil, T. Kim and N. A. M. Barakat, *RSC Adv.*, 2016, **6**, 104933.
7 Q. Yang, K. Y. Wang and T. S. Chung, *Environ. Sci. Technol.*, 2009, **43**, 2800–2805.
8 M. Amini, M. Jahanshahi and A. Rahimpour, *J. Membr. Sci.*, 2013, **435**, 233–241.
9 D. Qin, Z. Liu, H. Bai and D. D. Sun, *J. Mater. Chem. A*, 2017, **5**, 12183–12192.
10 N. Ma, J. Wei, S. Qi, Y. Zhao, Y. Gao and C. Y. Tang, *J. Membr. Sci.*, 2013, **441**, 54–62.
11 Y. Q. Wang, R. W. Ou, Q. Q. Ge, H. T. Wang and T. W. Xu, *Desalination*, 2013, **330**, 70–78.
12 J. W. Han, B. Kim, J. Li and M. Meyyappan, *RSC Adv.*, 2013, **4**, 549–553.
13 Z. Yu, G. Zeng, Y. Pan, L. Lv, H. Min, L. Zhang and Y. He, *RSC Adv.*, 2015, **5**, 75998–76006.
14 D. Emadzadeh, W. J. Lau, T. Matsuura, M. Rahbari-Sisakht and A. F. Ismail, *Chem. Eng. J.*, 2014, **237**, 70–80.
15 D. Emadzadeh, W. J. Lau and A. F. Ismail, *Desalination*, 2013, **330**, 90–99.
16 D. L. Shaffer, J. R. Werber, H. Jaramillo, S. Lin and M. Elimelech, *Desalination*, 2015, **356**, 271–284.
17 A. Achilli, T. Y. Cath, E. A. Marchand and A. E. Childress, *Desalination*, 2009, **239**, 10–21.
18 E. S. Kim and B. L. Deng, *J. Membr. Sci.*, 2011, **375**, 46–54.
19 H. Y. Zhao, S. Qiu, L. G. Wu, L. Zhang, H. L. Chen and C. J. Gao, *J. Membr. Sci.*, 2014, **450**, 249–256.
20 W. C. L. Lay, Y. Liu and A. G. Fane, *Water Res.*, 2010, **44**, 21–40.
21 N. Ma, J. Wei, R. Liao and C. Y. Tang, *J. Membr. Sci.*, 2012, **405–406**, 149–157.
22 K. P. Lee, T. C. Arnot and D. Mattia, *J. Membr. Sci.*, 2011, **370**, 1–22.
23 Y. Zeng, L. Qiu, K. Wang, J. Yao, D. Li, G. P. Simon, R. Wang and H. Wang, *RSC Adv.*, 2012, **3**, 887–894.
24 X. Li, K. Teng, J. Shi, W. Wang, Z. Xu, H. Deng, H. Lv and F. Li, *J. Taiwan Inst. Chem. Eng.*, 2016, **60**, 636–642.
25 M. Amini, A. Rahimpour and M. Jahanshahi, *Desalin. Water Treat.*, 2016, **57**, 14013–14023.
26 M. Yue, B. Zhou, K. Jiao, X. Qian, Z. Xu, K. Teng, L. Zhao, J. Wang and Y. Jiao, *Appl. Surf. Sci.*, 2015, **327**, 93–99.
27 T. Wu, B. Zhou, T. Zhu, J. Shi, Z. Xu, C. Hu and J. Wang, *RSC Adv.*, 2015, **5**, 7880–7889.
28 K. Jiao, T. Zhu, X. Li, M. Shan, Z. Xu and Y. Jiao, *J. Nanopart. Res.*, 2015, **17**, 1–15.
29 X. Song, L. Wang, C. Y. Tang, Z. Wang and C. Gao, *Desalination*, 2015, **369**, 1–9.
30 Y. Wang, R. Ou, Q. Ge, H. Wang and T. Xu, *Desalination*, 2013, **330**, 70–78.
31 H. M. Hegab, A. ElMekawy, T. G. Barclay, A. Michelmore, L. Zou, C. P. Saint and M. Ginic-Markovic, *ACS Appl. Mater. Interfaces*, 2015, **7**, 18004–18016.
32 H. M. Hegab, A. ElMekawy, T. G. Barclay, A. Michelmore, L. Zou, C. P. Saint and M. Ginic-Markovic, *Desalination*, 2016, **385**, 126–137.
33 M. J. Park, S. Phuntsho, T. He, G. M. Nisola, L. D. Tijing, X.-M. Li, G. Chen, W.-J. Chung and H. K. Shon, *J. Membr. Sci.*, 2015, **493**, 496–507.
34 L. Shen, S. Xiong and Y. Wang, *Chem. Eng. Sci.*, 2016, **143**, 194–205.
35 Y. Wang, R. Ou, H. Wang and T. Xu, *J. Membr. Sci.*, 2015, **475**, 281–289.
36 H. Salehi, M. Rastgar and A. Shakeri, *Appl. Surf. Sci.*, 2017, **413**, 99–108.
37 Z. Dabaghian and A. Rahimpour, *Chem. Eng. Res. Des.*, 2015, **104**, 647–657.
38 M. Ghanbari, D. Emadzadeh, W. J. Lau, S. O. Lai, T. Matsuura and A. F. Ismail, *Desalination*, 2015, **358**, 33–41.

39 M. Ghanbari, D. Emadzadeh, W. J. Lau, H. Riazi, D. Almasi and A. F. Ismail, *Desalination*, 2016, **377**, 152–162.
40 W. kuang, Z. Liu, H. Yu, G. Kang, X. Jie, Y. Jin and Y. Cao, *J. Membr. Sci.*, 2016, **497**, 485–493.
41 Q. Liu, J. Li, Z. Zhou, J. Xie and J. Y. Lee, *Sci. Rep.*, 2016, **6**, 19593.
42 N.-N. Bui and J. R. McCutcheon, *J. Membr. Sci.*, 2016, **518**, 338–346.
43 Y. Huang, H. Jin, P. Yu and Y. Luo, *Desalin. Water Treat.*, 2015, **57**, 20177–20187.
44 N. Niksefat, M. Jahanshahi and A. Rahimpour, *Desalination*, 2014, **343**, 140–146.
45 M. Obaid, Z. K. Ghouri, O. A. Fadali, K. A. Khalil, A. A. Almajid and N. A. Barakat, *ACS Appl. Mater. Interfaces*, 2016, **8**, 4561–4574.
46 Z. Liu and Y. Hu, *ACS Appl. Mater. Interfaces*, 2016, **8**, 21666–21673.
47 E. Yang, K.-J. Chae, A. B. Alayande, K.-Y. Kim and I. S. Kim, *J. Membr. Sci.*, 2016, **513**, 217–225.
48 D. Emadzadeh, W. J. Lau, T. Matsuura, N. Hilal and A. F. Ismail, *Desalination*, 2014, **348**, 82–88.
49 D. Emadzadeh, W. J. Lau, M. Rahbari-Sisakht, H. Ilbeygi, D. Rana, T. Matsuura and A. F. Ismail, *Chem. Eng. J.*, 2015, **281**, 243–251.
50 N. M. Mubarak, J. N. Sahu, E. C. Abdullah and N. S. Jayakumar, *Sep. Purif. Rev.*, 2014, **43**, 311–338.
51 P. S. Goh, B. C. Ng, W. J. Lau and A. F. Ismail, *Sep. Purif. Rev.*, 2014, **44**, 216–249.
52 R. Das, M. E. Ali, S. B. A. Hamid, S. Ramakrishna and Z. Z. Chowdhury, *Desalination*, 2014, **336**, 97–109.
53 Y. Wang, Z. Xu and L. Chen, *Appl. Mech. Mater.*, 2010, **44–47**, 2181–2185.
54 Y. Wang, L. Chen and Z. Xu, *Adv. Mater. Res.*, 2011, **150–151**, 1106–1109.
55 A. Kalra, S. Garde and G. Hummer, *Proc. Natl. Acad. Sci. U. S. A.*, 2003, **100**, 10175–10180.
56 Y. Chan and J. M. Hill, *J. Membr. Sci.*, 2011, **372**, 57–65.
57 X. F. Li, J. L. Yang, Y. H. Hu, J. J. Wang, Y. L. Li, M. Cai, R. Y. Li and X. L. Sun, *J. Mater. Chem.*, 2012, **22**, 18847–18853.
58 H. J. Wang, G. P. Yin, Y. Y. Shao, Z. B. Wang and Y. Z. Gao, *J. Power Sources*, 2008, **176**, 128–131.
59 S. Kar, R. C. Bindal and P. K. Tewari, *Nano Today*, 2012, **7**, 385–389.
60 H. J. Kim, Y. Baek, K. Choi, D. G. Kim, H. Kang, Y. S. Choi, J. Yoon and J. C. Lee, *RSC Adv.*, 2014, **4**, 32802–32810.
61 Y. X. Jia, H. L. Li, M. Wang, L. Y. Wu and Y. D. Hu, *Sep. Purif. Technol.*, 2010, **75**, 55–60.
62 H. Q. Wu, B. B. Tang and P. Y. Wu, *J. Membr. Sci.*, 2010, **362**, 374–383.
63 H. A. Shawky, S. R. Chae, S. H. Lin and M. R. Wiesner, *Desalination*, 2011, **272**, 46–50.
64 M. Endo, T. Hayashi, Y. A. Kim, M. Terrones and M. S. Dresselhaus, *Philos. Trans. R. Soc., A*, 2004, **362**, 2223–2238.
65 H. Y. Ma, C. Burger, B. S. Hsiao and B. Chu, *ACS Macro Lett.*, 2012, **1**, 723–726.
66 J. H. Choi, J. Jegal and W. N. Kim, *J. Membr. Sci.*, 2006, **284**, 406–415.
67 L. Dumee, J. Lee, K. Sears, B. Tardy, M. Duke and S. Gray, *J. Membr. Sci.*, 2013, **427**, 422–430.
68 H. L. Li, Y. X. Jia and Y. D. Hu, *Acta Phys.-Chim. Sin.*, 2012, **28**, 573–577.
69 Z. Zhao, K. Teng, N. Li, X. Li, Z. Xu, L. Chen, J. Niu, H. Fu, L. Zhao and Y. Liu, *Compos. Struct.*, 2017, **159**, 761–772.
70 Y. Li and M. Kroger, *Carbon*, 2012, **50**, 1793–1806.
71 A. Deneuve, K. Wang, I. Janowska, K. Chizari, D. Edouard, O. Ersen, M. J. Ledoux and C. Pham-Huu, *Appl. Catal., A*, 2011, **400**, 230–237.
72 L. F. Dumee, K. Sears, J. Schutz, N. Finn, C. Huynh, S. Hawkins, M. Duke and S. Gray, *J. Membr. Sci.*, 2010, **351**, 36–43.
73 L. Dumee, K. Sears, J. Schutz, N. Finn, M. Duke and S. Gray, *Desalin. Water Treat.*, 2010, **17**, 72–79.
74 L. Dumee, V. Germain, K. Sears, J. Schutz, N. Finn, M. Duke, S. Cerneaux, D. Cornu and S. Gray, *J. Membr. Sci.*, 2011, **376**, 241–246.
75 L. F. Chen, H. Q. Xie, Y. Li and W. Yu, *Mater. Lett.*, 2009, **63**, 45–47.
76 A. Villa, M. Plebani, M. Schiavoni, C. Milone, E. Piperopoulos, S. Galvagno and L. Prati, *Catal. Today*, 2012, **186**, 76–82.
77 K. Sears, L. Dumee, J. Schutz, M. She, C. Huynh, S. Hawkins, M. Duke and S. Gray, *Materials*, 2010, **3**, 127–149.
78 R. L. D. Whitby, S. V. Mikhalovsky and V. M. Gun'ko, *Carbon*, 2010, **48**, 145–152.
79 L. Dumée, J. Lee, K. Sears, B. Tardy, M. Duke and S. Gray, *J. Membr. Sci.*, 2013, **427**, 422–430.
80 M. Hu and B. X. Mi, *Environ. Sci. Technol.*, 2013, **47**, 3715–3723.
81 Z. Xu, Y. Zhang, X. Qian, J. Shi, L. Chen, B. Li, J. Niu and L. Liu, *Appl. Surf. Sci.*, 2014, **316**, 308–314.
82 Y. Han, Z. Xu and C. Gao, *Adv. Funct. Mater.*, 2013, **23**, 3693–3700.
83 Y. Q. Sun, Q. O. Wu and G. Q. Shi, *Energy Environ. Sci.*, 2011, **4**, 1113–1132.
84 Z. Xu, J. Zhang, M. Shan, Y. Li, B. Li, J. Niu, B. Zhou and X. Qian, *J. Membr. Sci.*, 2014, **458**, 1–13.
85 L. Chen, X. Li, L. Wang, W. Wang and Z. Xu, *Polym. Compos.*, 2017, **38**, 236–247.
86 J. Lee, H. R. Chae, Y. J. Won, K. Lee, C. H. Lee, H. H. Lee, I. C. Kim and J. M. Lee, *J. Membr. Sci.*, 2013, **448**, 223–230.
87 B. X. Mi, *Science*, 2014, **343**, 740–742.
88 F. Perreault, M. E. Tousley and M. Elimelech, *Environ. Sci. Technol. Lett.*, 2014, **1**, 71–76.
89 S. Zinadini, A. A. Zinatizadeh, M. Rahimi, V. Vatanpour and H. Zangeneh, *J. Membr. Sci.*, 2014, **453**, 292–301.
90 H. Y. Zhao, L. G. Wu, Z. J. Zhou, L. Zhang and H. L. Chen, *Phys. Chem. Chem. Phys.*, 2013, **15**, 9084–9092.
91 Z. W. Xu, J. G. Zhang, M. J. Shan, Y. L. Li, B. D. Li, J. R. Niu, B. M. Zhou and X. M. Qian, *J. Membr. Sci.*, 2014, **458**, 1–13.
92 J. Q. Wang, P. Zhang, B. Liang, Y. X. Liu, T. Xu, L. F. Wang, B. Cao and K. Pan, *ACS Appl. Mater. Interfaces*, 2016, **8**, 6211–6218.

93 A. Akbari, P. Sheath, S. T. Martin, D. B. Shinde, M. Shaibani, P. C. Banerjee, R. Tkacz, D. Bhattacharyya and M. Majumder, *Nat. Commun.*, 2016, **7**, 12.
94 S. J. Gao, H. L. Qin, P. P. Liu and J. Jin, *J. Mater. Chem. A*, 2015, **3**, 6649–6654.
95 M. Li, J. Shi, C. Chen, N. Li, Z. Xu, J. Li, H. Lv, X. Qian and X. Jiao, *J. Nanopart. Res.*, 2017, 19.
96 Y. Han, Y. Q. Jiang and C. Gao, *ACS Appl. Mater. Interfaces*, 2015, **7**, 8147–8155.
97 P. Z. Sun, Q. Chen, X. D. Li, H. Liu, K. L. Wang, M. L. Zhong, J. Q. Wei, D. H. Wu, R. Z. Ma, T. Sasaki and H. W. Zhu, *NPG Asia Mater.*, 2015, **7**, 8.
98 P. Sun, R. Ma, H. Deng, Z. Song, Z. Zhen, K. Wang, T. Sasaki, Z. Xu and H. Zhu, *Chem. Sci.*, 2016, **7**, 6988–6994.
99 Y. J. Zhang, T. Mori, L. Niu and J. H. Ye, *Energy Environ. Sci.*, 2011, **4**, 4517–4521.
100 Y. Hou, Z. H. Wen, S. M. Cui, X. R. Guo and J. H. Chen, *Adv. Mater.*, 2013, **25**, 6291–6297.
101 Y. Joo, Y. Jeon, S. U. Lee, J. H. Sim, J. Ryu, S. Lee, H. Lee and D. Sohn, *J. Phys. Chem. C*, 2012, **116**, 18230–18235.
102 Y. F. Chen, Y. T. Zhang, H. Q. Zhang, J. D. Liu and C. H. Song, *Chem. Eng. J.*, 2013, **228**, 12–20.
103 Y. S. Liu, X. Q. Jiang, B. J. Li, X. D. Zhang, T. Z. Liu, X. S. Yan, J. Ding, Q. Cai and J. M. Zhang, *J. Mater. Chem. A*, 2014, **2**, 4264–4269.
104 C. P. Li, J. Q. Wang, S. Q. Feng, Z. L. Yang and S. J. Ding, *J. Mater. Chem. A*, 2013, **1**, 8045–8054.
105 R. Wang, L. Shi, C. Y. Y. Tang, S. R. Chou, C. Qiu and A. G. Fane, *J. Membr. Sci.*, 2010, **355**, 158–167.
106 G. Hota, B. R. Kumar, W. J. Ng and S. Ramakrishna, *J. Mater. Sci.*, 2007, **43**, 212–217.
107 L. Y. Yu, Z. L. Xu, H. M. Shen and H. Yang, *J. Membr. Sci.*, 2009, **337**, 257–265.
108 J. W. Cho and K. I. Sul, *Polymer*, 2001, **42**, 727–736.
109 T. Ogoshi and Y. Chujo, *J. Polym. Sci., Part A: Polym. Chem.*, 2005, **43**, 3543–3550.
110 M. Baghbanzadeh, A. Rashidi, D. Rashtchian, R. Lotfi and A. Amrollahi, *Thermochim. Acta*, 2012, **549**, 87–94.
111 J. Vega-Baudrit, V. Navarro-Banon, P. Vazquez and J. M. Martin-Martinez, *Int. J. Adhes. Adhes.*, 2006, **26**, 378–387.
112 X. F. Yao, D. Zhou and H. Y. Yeh, *Aerosp. Sci. Technol.*, 2008, **12**, 223–230.
113 S. Sprenger, *J. Appl. Polym. Sci.*, 2013, **130**, 1421–1428.
114 X. Wang, L. Wang, Q. Su and J. P. Zheng, *Compos. Sci. Technol.*, 2013, **89**, 52–60.
115 O. Malay, O. Oguz, C. Kosak, E. Yilgor, I. Yilgor and Y. Z. Menceloglu, *Polymer*, 2013, **54**, 5310–5320.
116 J. Yang and J. J. Zhao, *Mater. Lett.*, 2014, **120**, 36–38.
117 Y. L. Liu, C. Y. Hsu, W. L. Wei and R. J. Jeng, *Polymer*, 2003, **44**, 5159–5167.
118 W. D. Liu, B. K. Zhu, J. Zhang and Y. Y. Xu, *Polym. Adv. Technol.*, 2007, **18**, 522–528.
119 H. Palza, R. Vergara and P. Zapata, *Compos. Sci. Technol.*, 2011, **71**, 535–540.
120 G. Bissadi and B. Kruczek, *J. Therm. Anal. Calorim.*, 2014, **117**, 73–83.
121 I. Ab Rahman and V. Padavettan, *J. Nanomater.*, 2012, 132424.
122 X. X. Song, Z. Y. Liu and D. Sun, *Adv. Mater.*, 2011, **23**, 3256–3260.
123 F. Dorosti, M. R. Omidkhah, M. Z. Pedram and F. Moghadam, *Chem. Eng. J.*, 2011, **171**, 1469–1476.
124 A. J. J. Koekkoek, J. A. R. van Veen, P. B. Gerrtisen, P. Giltay, P. Magusin and E. J. M. Hensen, *Microporous Mesoporous Mater.*, 2012, **151**, 34–43.
125 S. L. Suib, *Science*, 2003, **302**, 1335–1336.
126 S. H. Kim, S. Y. Kwak, B. H. Sohn and T. H. Park, *J. Membr. Sci.*, 2003, **211**, 157–165.
127 B. H. Jeong, E. M. V. Hoek, Y. S. Yan, A. Subramani, X. F. Huang, G. Hurwitz, A. K. Ghosh and A. Jawor, *J. Membr. Sci.*, 2007, **294**, 1–7.
128 M. L. Lind, A. K. Ghosh, A. Jawor, X. F. Huang, W. Hou, Y. Yang and E. M. V. Hoek, *Langmuir*, 2009, **25**, 10139–10145.
129 M. L. Lind, D. E. Suk, T. V. Nguyen and E. M. V. Hoek, *Environ. Sci. Technol.*, 2010, **44**, 8230–8235.
130 H. Y. Liu, L. L. Liu, C. L. Yang, Z. H. Li, Q. Z. Xiao, G. T. Lei and Y. H. Ding, *Electrochim. Acta*, 2014, **121**, 328–336.
131 Y. Q. Zhang, X. Bin Yang, Z. X. Wang, J. Long and L. Shao, *J. Mater. Chem. A*, 2017, **5**, 7316–7325.
132 X. B. Yang, X. Jiang, Y. D. Huang, Z. H. Guo and L. Shao, *ACS Appl. Mater. Interfaces*, 2017, **9**, 5590–5599.
133 X. Q. Cheng, K. Konstas, C. M. Doherty, C. D. Wood, X. Mulet, Z. L. Xie, D. Ng, M. R. Hill, L. Shao and C. H. Lau, *ACS Appl. Mater. Interfaces*, 2017, **9**, 14401–14408.
134 J. Y. Bottero, M. Auffan, J. Rose, C. Mouneyrac, C. Botta, J. Labille, A. Masion, A. Thill and C. Chaneac, *C. R. Geosci.*, 2011, **343**, 168–176.
135 X. M. Wang, X. Y. Li and K. M. Shih, *J. Membr. Sci.*, 2011, **368**, 134–143.
136 H. Wu, J. Mansouri and V. Chen, *J. Membr. Sci.*, 2013, **433**, 135–151.
137 Q. L. Li, S. Mahendra, D. Y. Lyon, L. Brunet, M. V. Liga, D. Li and P. J. J. Alvarez, *Water Res.*, 2008, **42**, 4591–4602.
138 S. J. Klaine, P. J. J. Alvarez, G. E. Batley, T. F. Fernandes, R. D. Handy, D. Y. Lyon, S. Mahendra, M. J. McLaughlin and J. R. Lead, *Environ. Toxicol. Chem.*, 2008, **27**, 1825–1851.
139 A. Mollahosseini, A. Rahimpour, M. Jahamshahi, M. Peyravi and M. Khavarpour, *Desalination*, 2012, **306**, 41–50.
140 K. Zodrow, L. Brunet, S. Mahendra, D. Li, A. Zhang, Q. L. Li and P. J. J. Alvarez, *Water Res.*, 2009, **43**, 715–723.
141 M. Herzberg and M. Elimelech, *J. Membr. Sci.*, 2007, **295**, 11–20.
142 Y. Li, J. H. Ho and C. P. Ooi, *Mater. Sci. Eng., C*, 2010, **30**, 1137–1144.
143 F. Diagne, R. Malaisamy, V. Boddie, R. D. Holbrook, B. Eribo and K. L. Jones, *Environ. Sci. Technol.*, 2012, **46**, 4025–4033.
144 J. S. Taurozzi, H. Arul, V. Z. Bosak, A. F. Burban, T. C. Voice, M. L. Bruening and V. V. Tarabara, *J. Membr. Sci.*, 2008, **325**, 58–68.

145 J. Huang, G. Arthanareeswaran and K. S. Zhang, *Desalination*, 2012, **285**, 100–107.
146 S. Y. Lee, H. J. Kim, R. Patel, S. J. Im, J. H. Kim and B. R. Min, *Polym. Adv. Technol.*, 2007, **18**, 562–568.
147 H. L. Yang, J. C. T. Lin and C. Huang, *Water Res.*, 2009, **43**, 3777–3786.
148 X. Liu, S. Qi, Y. Li, L. Yang, B. Cao and C. Y. Tang, *Water Res.*, 2013, **47**, 3081–3092.
149 L. Djafer, A. Ayral and A. Ouagued, *Sep. Purif. Technol.*, 2010, **75**, 198–203.
150 A. Rahimpour, M. Jahanshahi, A. Mollahosseini and B. Rajaeian, *Desalination*, 2012, **285**, 31–38.
151 Z. Xu, T. Wu, J. Shi, K. Teng, W. Wang, M. Ma, J. Li, X. Qian, C. Li and J. Fan, *J. Membr. Sci.*, 2016, **520**, 281–293.
152 Q. Q. Wang, X. T. Wang, Z. H. Wang, J. Huang and Y. Wang, *J. Membr. Sci.*, 2013, **442**, 57–64.
153 Y. H. Teow, A. L. Ahmad, J. K. Lim and B. S. Ooi, *J. Appl. Polym. Sci.*, 2013, **128**, 3184–3192.
154 G. Ghasemzadeh, M. Momenpour, F. Omidi, M. R. Hosseini, M. Ahani and A. Barzegari, *Front. Environ. Sci. Eng.*, 2014, **8**, 471–482.
155 Z. Xu, X. Li, W. Wang, J. Shi, K. Teng, X. Qian, M. Shan, C. Li, C. Yang and L. Liu, *Ceram. Int.*, 2016, **42**, 15012–15022.
156 X. Cheng, S. Ding, J. Guo, C. Zhang, Z. Guo and L. Shao, *J. Membr. Sci.*, 2017, **536**, 19–27.
157 N. A. A. Hamid, A. F. Ismail, T. Matsuura, A. W. Zularisam, W. J. Lau, E. Yuliwati and M. S. Abdullah, *Desalination*, 2011, **273**, 85–92.
158 A. W. Zularisam, A. F. Ismail, M. R. Salim, M. Sakinah and H. Ozaki, *Desalination*, 2007, **212**, 191–208.
159 A. Nguyen, L. D. Zou and C. Priest, *J. Membr. Sci.*, 2014, **454**, 264–271.
160 M. Amini, A. Rahimpour and M. Jahanshahi, *Desalin. Water Treat.*, 2016, **57**, 14013–14023.
161 J. Kim and B. Van der Bruggen, *Environ. Pollut.*, 2010, **158**, 2335–2349.
162 P. S. Tin, T. S. Chung, L. Y. Jiang and S. Kulprathipanja, *Carbon*, 2005, **43**, 2025–2027.
163 J. N. Shen, H. M. Ruan, L. G. Wu and C. J. Gao, *Chem. Eng. J.*, 2011, **168**, 1272–1278.
164 J. n. Shen, C. c. Yu, H. m. Ruan, C. j. Gao and B. Van der Bruggen, *J. Membr. Sci.*, 2013, **442**, 18–26.
165 M. Ghanbari, D. Emadzadeh, W. J. Lau, T. Matsuura, M. Davoody and A. F. Ismail, *Desalination*, 2015, **371**, 104–114.
166 R. Zhang, Y. Su, X. Zhao, Y. Li, J. Zhao and Z. Jiang, *J. Membr. Sci.*, 2014, **470**, 9–17.
167 P. S. Zhong, N. Widjojo, T. S. Chung, M. Weber and C. Maletzko, *J. Membr. Sci.*, 2012, **417**, 52–60.
168 P. T. Hammond, *Curr. Opin. Colloid Interface Sci.*, 1999, **4**, 430–442.
169 R. Malaisamy and M. L. Bruening, *Langmuir*, 2005, **21**, 10587–10592.
170 O. Y. Lu, R. Malaisamy and M. L. Bruening, *J. Membr. Sci.*, 2008, **310**, 76–84.
171 Q. Saren, C. Q. Qiu and C. Y. Y. Tang, *Environ. Sci. Technol.*, 2011, **45**, 5201–5208.
172 S. Qi, C. Q. Qiu, Y. Zhao and C. Y. Tang, *J. Membr. Sci.*, 2012, **405–406**, 20–29.
173 C. Qiu, S. Qi and C. Y. Tang, *J. Membr. Sci.*, 2011, **381**, 74–80.
174 M. Herzberg, S. Kang and M. Elimelech, *Environ. Sci. Technol.*, 2009, **43**, 4393–4398.
175 P. Bertrand, A. Jonas, A. Laschewsky and R. Legras, *Macromol. Rapid Commun.*, 2000, **21**, 319–348.
176 S. Zhao, L. Zou, C. Y. Tang and D. Mulcahy, *J. Membr. Sci.*, 2012, **396**, 1–21.
177 X. Qu, P. J. Alvarez and Q. Li, *Water Res.*, 2013, **47**, 3931–3946.
178 M. M. Ling and T. S. Chung, *Desalination*, 2011, **278**, 194–202.
179 L. Chekli, S. Phuntsho, H. K. Shon, S. Vigneswaran, J. Kandasamy and A. Chanan, *Desalin. Water Treat.*, 2012, **43**, 167–184.
180 T. S. Chung, S. Zhang, K. Y. Wang, J. Su and M. M. Ling, *Desalination*, 2012, **287**, 78–81.
181 A. Soroush, W. Ma, Y. Silvino and M. S. Rahaman, *Environ. Sci.: Nano*, 2015, **2**, 395–405.
182 D. N. Wang, X. F. Li, J. J. Wang, J. L. Yang, D. S. Geng, R. Y. Li, M. Cai, T. K. Sham and X. L. Sun, *J. Phys. Chem. C*, 2012, **116**, 22149–22156.
183 C. Matranga, B. Bockrath, N. Chopra, B. J. Hinds and R. Andrews, *Langmuir*, 2006, **22**, 1235–1240.
184 J. K. Holt, H. G. Park, Y. M. Wang, M. Stadermann, A. B. Artyukhin, C. P. Grigoropoulos, A. Noy and O. Bakajin, *Science*, 2006, **312**, 1034–1037.
185 B. J. Hinds, N. Chopra, T. Rantell, R. Andrews, V. Gavalas and L. G. Bachas, *Science*, 2004, **303**, 62–65.
186 J. J. Wang, G. P. Yin, Y. G. Chen, R. Y. Li and X. L. Sun, *Int. J. Hydrogen Energy*, 2009, **34**, 8270–8275.
187 K. Dasgupta, S. Kar, R. Venugopalan, R. C. Bindal, S. Prabhakar, P. K. Tewari, S. Bhattacharya, S. K. Gupta and D. Sathiyamoorthy, *Mater. Lett.*, 2008, **62**, 1989–1992.
188 S. Kar, R. C. Bindal, S. Prabhakar, P. K. Tewari, K. Dasgupta and D. Sathiyamoorthy, *Int. J. Nucl. Desalin.*, 2008, **3**, 143–150.
189 P. Sabbatini, F. Yrazu, F. Rossi, G. Thern, A. Marajofsky and M. M. F. de Cortalezzi, *Water Res.*, 2010, **44**, 5702–5712.
190 V. Vatanpour, S. S. Madaeni, R. Moradian, S. Zinadini and B. Astinchap, *J. Membr. Sci.*, 2011, **375**, 284–294.
191 Z. Xu, T. Wu, J. Shi, W. Wang, K. Teng, X. Qian, M. Shan, H. Deng, X. Tian, C. Li and F. Li, *ACS Appl. Mater. Interfaces*, 2016, **8**, 18418–18429.